MAJOR ARTICLE

Granuloma Correlates of Protection Against Tuberculosis and Mechanisms of Immune Modulation by *Mycobacterium tuberculosis*

Smriti Mehra,[1] Xavier Alvarez,[2] Peter J. Didier,[2] Lara A. Doyle,[3] James L. Blanchard,[3] Andrew A. Lackner,[2,5] and Deepak Kaushal[4,5]

[1]Division of Microbiology, [2]Division of Comparative Pathology, [3]Division of Veterinary Medicine, and [4]Division of Bacteriology and Parasitology, Tulane National Primate Research Center, Covington, Louisiana; and [5]Tulane University School of Medicine, New Orleans, Louisiana

Background. The BCG vaccine is ineffective against adult tuberculosis. Hence, new antituberculosis vaccines are needed. Correlates of protection against tuberculosis are not known. We studied the effects of BCG vaccination on gene expression in tuberculosis granulomas using macaques.

Methods. Macaques were BCG-vaccinated or sham-vaccinated and then challenged with virulent *Mycobacterium tuberculosis*. Lung lesions were used for comparative transcriptomics.

Results. Vaccinated macaques were protected with lower bacterial burden and immunopathology. Lesions from BCG-vaccinated nonhuman primates (NHPs) showed a better balance of α- and β-chemokine gene expression with higher levels of β-chemokine expression relative to nonvaccinated animals. Consistent with this, sham-vaccinated macaques recruited fewer macrophages relative to neutrophils in their lungs. The expression of indoleamine 2,3-dioxygenase (IDO), a known immunosuppressor, was significantly higher in both week 5 and 10 lesions from sham-vaccinated, relative to BCG-vaccinated, NHPs. IDO expression was primarily limited to the nonlymphocytic region of the lesions, within the inner ring structure surrounding the central necrosis.

Conclusions. Our study defines lung gene expression correlates of protective response against tuberculosis, relative to disease, which can potentially be employed to assess the efficacy of candidate antituberculosis vaccines. *Mycobacterium tuberculosis* may modulate protective immune responses using diverse mechanisms, including increased recruitment of inflammatory neutrophils and the concomitant use of IDO to modulate inflammation.

Keywords. *Mycobacterium tuberculosis*; transcriptomics; IDO.

Tuberculosis is responsible for the death of >1.5 million people every year [1]. The BCG vaccine provides protection from childhood tuberculosis but is ineffective against adult pulmonary infection [2, 3]. Hence, new and effective antituberculosis vaccines are urgently required. However, the true correlates of protection against tuberculosis vis-à-vis infection are not well understood.

The prototypical response to infection with *Mycobacterium tuberculosis* is the formation of a granuloma [4]. While containing the spread of *Mycobacterium tuberculosis,* granulomas also provide it with an environment to persist [5]. Therefore, the study of tuberculosis granulomas provides insight into crucial host–pathogen interactions [4]. It is difficult to perform such studies in human samples because of variability in dose and pathogenicity; genetic, geographic, and racial diversity in patients; time elapsed since infection; the number of reinfection events; coinfection; and other confounding factors.

Nonhuman primates (NHPs) are excellent models of human tuberculosis. It is possible to model progression to latency, reactivation, and human-like granuloma architecture in NHPs experimentally infected with *Mycobacterium tuberculosis* (reviewed in [6, 7]). Rhesus macaque tuberculosis granulomas exhibit a massive reprogramming of the initial proinflammatory transcriptomic surge at the chronic stage [8]. Studies

Received 9 July 2012; accepted 10 August 2012; electronically published 18 December 2012.

Correspondence: Deepak Kaushal, PhD, Tulane National Primate Research Center, 18703 Three Rivers Rd, Covington, LA 70433 (dkaushal@tulane.edu).

The Journal of Infectious Diseases 2013;207:1115–27

DOI: 10.1093/infdis/jis778

in NHPs show that that BCG can protect against severe tuberculosis [9, 10]. We therefore hypothesized that the direct comparison of granulomas from NHPs protected by BCG vaccination to those not protected could allow us to better understand the requirements of protection. These comparisons would potentially highlight, at the gene expression level, the differences in tuberculosis granulomas that successfully contain bacterial replication from those that fail to check it. We infected BCG-vaccinated or sham-vaccinated NHPs with virulent *Mycobacterium tuberculosis* and studied granuloma gene expression at 2 different stages of infection. Our results identify potential correlates of protection, and indicate that the progression of *Mycobacterium tuberculosis* infection interferes with the expression of macrophage and lymphocyte chemoattractants, allowing a relatively greater number of neutrophils to accumulate in the lesions of animals with acute tuberculosis. The expression of indoleamine 2,3-dioxygenase (IDO) is highly induced in the region adjoining central necrosis (the ring wall), an area devoid of lymphocytes. IDO is a powerful immunosuppressant and thus may inhibit the access of lymphocytes to the central region of the granulomas.

MATERIALS AND METHODS

Animals

Four *Mycobacterium tuberculosis*-free, retrovirus-free, cynomolgus macaques were intradermally injected with 1×10^6 colony-forming units (CFU) of BCG-Danish in 1 mL Sauton media, whereas 4 animals received media only. The animals were infected with *Mycobacterium tuberculosis* Erdman 17 weeks postvaccination via intratracheal bronchoscopy into the right lower lobe [10, 11], and correlates of infection were obtained as described previously [12–14]. Body temperatures and weight were obtained weekly as part of a physical examination by board-certified clinical veterinarians and compared to pre-infection levels. Chest radiographs (CXRs) were read in a blinded fashion by 2 clinical veterinarians and scored using the following criteria: 0, no disease; 1, moderate involvement; 2, extensive involvement; 3, miliary tuberculosis. *Mycobacterium tuberculosis* load was determined by random sectioning and homogenization of lung followed by the MycoPrep method for decontamination [12–14]. Two NHPs from each group were necropsied 5 and 10 weeks after *Mycobacterium tuberculosis* infection as described earlier [12–14].

All animals were routinely cared for according to the guidelines prescribed by the National Institutes of Health Guide to Laboratory Animal Care. Humane endpoints were predefined in this protocol and applied as a measure of reduction of discomfort. All procedures were approved by Tulane National Primate Research Center, Institutional Animal Care and Use Committee, and the Tulane Institutional Biosafety Committee. The Tulane National Primate Research Center facilities are accredited by the American Association for Accreditation of Laboratory Animal Care and licensed by the US Department of Agriculture.

Transcriptomics

Three surgically excised granulomas from each macaque were pooled and transcriptome profiled relative to the total pool of normal lung tissue as described elsewhere [8, 14, 15]. Data were analyzed as described earlier [14–16] using Lowess-based normalization, and statistical significance was determined with the use of Spotfire DecisionSite [16]. Genes with levels of induction or repression <2-fold relative to normal lung were loaded onto DAVID (Database for Annotation, Visualization and Integrated Discovery, version 6.7; http://david.abcc.ncifcrf.gov/) to identify gene families with significant overrepresentation.

Confocal Microscopy

Multilabel confocal microscopy was performed as described earlier [8, 12–14]. Macrophages and neutrophils were detected using mouse anti-CD68–647 conjugate (catalog no. sc-20060, Santa Cruz Biotechnology, 1:10) and MAC387 (mouse, Dako, catalog no. M0747, 1:50) respectively. IDO was detected using a rabbit antibody (catalog no. HPA023072, Sigma; 1:400). Ten images of each slide were used for image analysis (Inform, PerkinElmer).

Statistics

Statistical significance was determined using either a 1-way analysis of variance with Bonferroni correction or a *t* test, within Prism version 5.01 (GraphPad).

RESULTS

Progression of Tuberculosis in BCG-Vaccinated Relative to Sham-Vaccinated NHPs

No adverse effects were observed following intradermal BCG vaccination of macaques. Between 4 and 8 weeks postvaccination, all BCG-vaccinated, but none of the sham-vaccinated animals, showed a positive tuberculin skin test. All 8 animals exhibited a positive tuberculin skin test at week 5 after *Mycobacterium tuberculosis* infection, indicating comparable infection.

Prior BCG vaccination significantly protected macaques against a lethal challenge with virulent *Mycobacterium tuberculosis* and produced significantly stunted tuberculosis. The control group exhibited a significant increase in body temperature at weeks 3 and 5 after *Mycobacterium tuberculosis* infection, relative to the BCG-vaccinated group (Figure 1*A*). The sham-vaccinated animals also showed significantly greater weight loss, relative to the BCG-vaccinated group (Figure 1*B*). The difference between the 2 groups was statistically significant during weeks 4–10. The sera of BCG-vaccinated animals

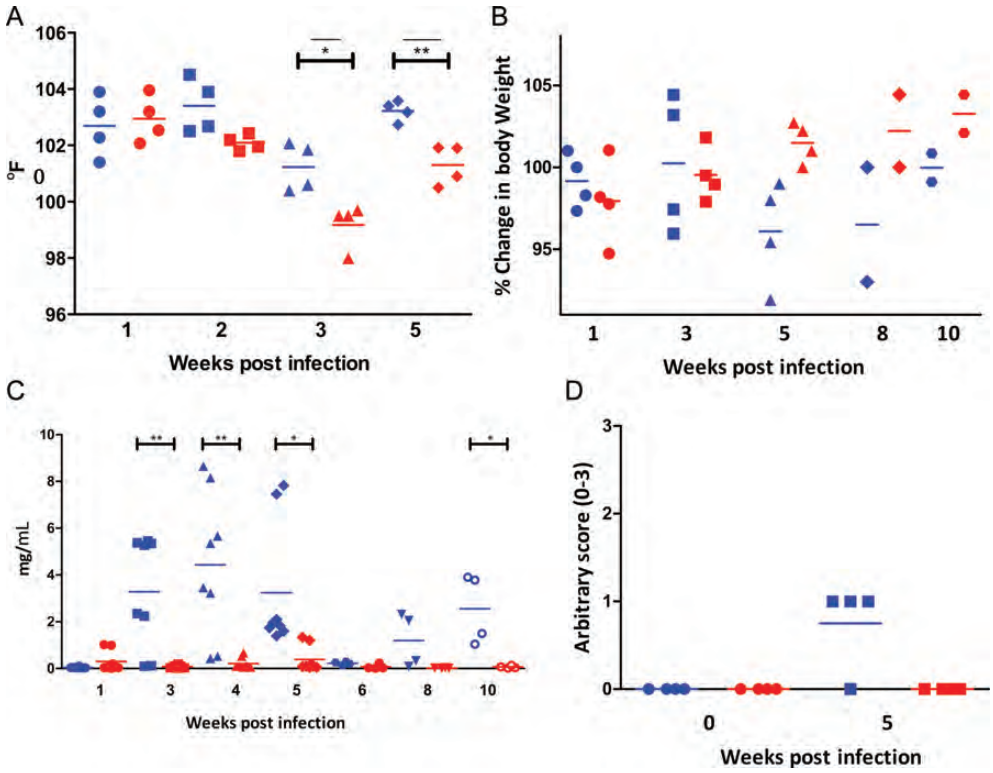

Figure 1. Comparison of clinical progression of disease in sham- and BCG-vaccinated nonhuman primates (NHPs). Blue symbols represent sham-vaccinated *Mycobacterium tuberculosis*-infected NHPs and red symbols represent BCG-vaccinated, *Mycobacterium tuberculosis*–infected NHPs. *A*, Changes in body temperature, expressed as degrees Fahrenheit. Circles: week 1; squares: week 3; triangles: week 4; diamonds: week 5. *B*, Changes in body weight, expressed as percentage of total weight at the time of *Mycobacterium tuberculosis* infection. Circles: week 1; squares: week 3; triangles: week 5; diamonds: week 8; hexagons: week 10. *C*, Changes in serum C-reactive protein levels. Circles: week 1; squares: week 3; triangles: week 4; diamonds: week 5; hexagons: week 6; downward triangles: week 8; open circles: week 10 (2 measurements per animal per time point). *D*, Changes in arbitrary chest radiographic (CXR) scores. X-axis denotes time in weeks post-*Mycobacterium tuberculosis* infection. Circles: week 1; squares: week 5. CXR scores were determined as described earlier [12–14], in a blinded fashion using the following scoring criteria: 0: normal; 1: moderate involvement; 2: extensive involvement; 3: miliary tuberculosis.

contained significantly lower levels of acute-phase marker C-reactive protein when compared to their sham-vaccinated counterparts (Figure 1*C*). CXRs corroborated the clinical differences in the progression of tuberculosis between the 2 groups of NHPs. Sham-vaccinated animals had significantly higher scores in their CXRs obtained 5 weeks postinfection, relative to BCG-vaccinated ones (Figure 1*D*).

Consistent with the clinical progression of disease in the 2 groups, the total *Mycobacterium tuberculosis* burden in lungs was significantly lower in the BCG-vaccinated NHPs relative to those that were sham-vaccinated, as evidenced from the temporal *Mycobacterium tuberculosis* burden in bronchoalveolar lavage fluid (Figure 2*A*) and bronchial lymph nodes (Figure 2*B*), as well as terminal lung tissue (Figure 2*C* and 2*D*). A higher level of bacterial CFU was present in the right (Figure 2*C*), relative to the left, lung (Figure 2*D*), as the initial inoculum was placed in the lower right lobe of the animals. Further, BCG significantly reduced the burden of *Mycobacterium tuberculosis* growth in extrathoracic tissues such as spleen (Figure 2*E*), liver, and kidney (not shown), relative to the NHPs that received placebo. Hence, BCG limits the extrapulmonary transmission of *Mycobacterium tuberculosis* in primates.

Lung-pathology analyses were in agreement with the clinical and bacteriological measures (Figure 3). Lesions in BCG-vaccinated areas were fewer and were largely limited to the lower right lobes, the site of initial inoculation with *Mycobacterium tuberculosis*, both upon gross pathologic (Figure 3*A* and 3*C*) and histopathologic (Figure 3*E* and 3*G*) analyses. In contrast, significantly more lesions and areas of consolidation were present in the sham-vaccinated group (Figure 3*B* and 3*D*; 3*F* and 3*H*). Significant differences were observed between the 2 groups of animals for total pathology scores (Figure 3*I*). Within individual lobes, the pathology scores were not significantly different for the inoculation site. However the total

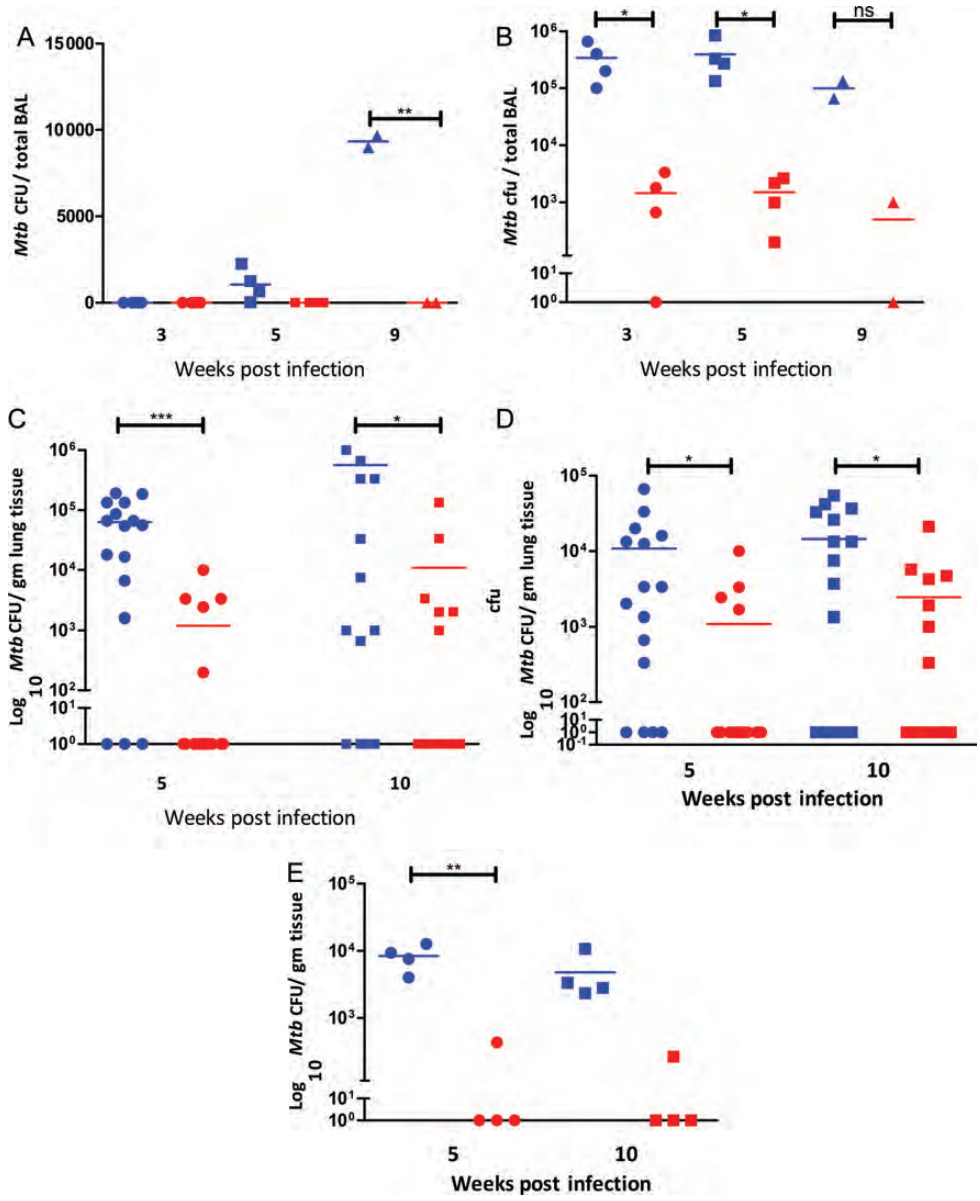

Figure 2. Comparison of bacterial burden in sham- and BCG-vaccinated nonhuman primates (NHPs). Blue symbols represent sham-vaccinated, *Mycobacterium tuberculosis*–infected NHPs, and red symbols represent BCG-vaccinated, *Mycobacterium tuberculosis*-infected NHPs. *A*, Temporal *Mycobacterium tuberculosis* colony-forming units (CFU) in bronchoalveolar lavage fluid (80 mL). Circles: week 3; squares: week 5; triangles: week 9. X-axis: time postinfection. Y-axis: numeric scale. *B*, Temporal *Mycobacterium tuberculosis* CFU in bronchial lymph nodes (per gram of tissue). Circles: week 3; squares: week 5; triangles: week 9. X-axis: time postinfection. Y-axis: $\log_{10}$ scale. *C*, *Mycobacterium tuberculosis* CFU in right lung (site of inoculation) at necropsy (per gram of tissue). Circles: week 5; squares: week 10. X-axis: time postinfection. Y-axis: $\log_{10}$ scale. *D*, *Mycobacterium tuberculosis* CFU in left lung (contralateral lobe) at necropsy (per gram of tissue). Circles: week 5; squares: week 10. X-axis: time postinfection. Y-axis: $\log_{10}$ scale. *E*, *Mycobacterium tuberculosis* CFU in spleen at necropsy (per gram of tissue). Circles: week 5; squares: week 10. X-axis: time postinfection. Y-axis: $\log_{10}$ scale. Abbreviations: BAL, bronchoalveolar lavage; CFU, colony-forming units.

differences and those for all the other lobes were significant (Figure 3*J*).

The clinical, microbiologic, and pathologic readouts described above clearly demonstrate the effectiveness of the protection imparted by BCG vaccination against challenge with highly virulent *Mycobacterium tuberculosis*. These results are consistent with those obtained in earlier studies with both cynomolgus [9] and rhesus [10] macaques.

Gene Expression in Early NHP Granulomas

Lung granulomas were obtained at necropsy from 2 sham-vaccinated *Mycobacterium tuberculosis*-infected NHPs and

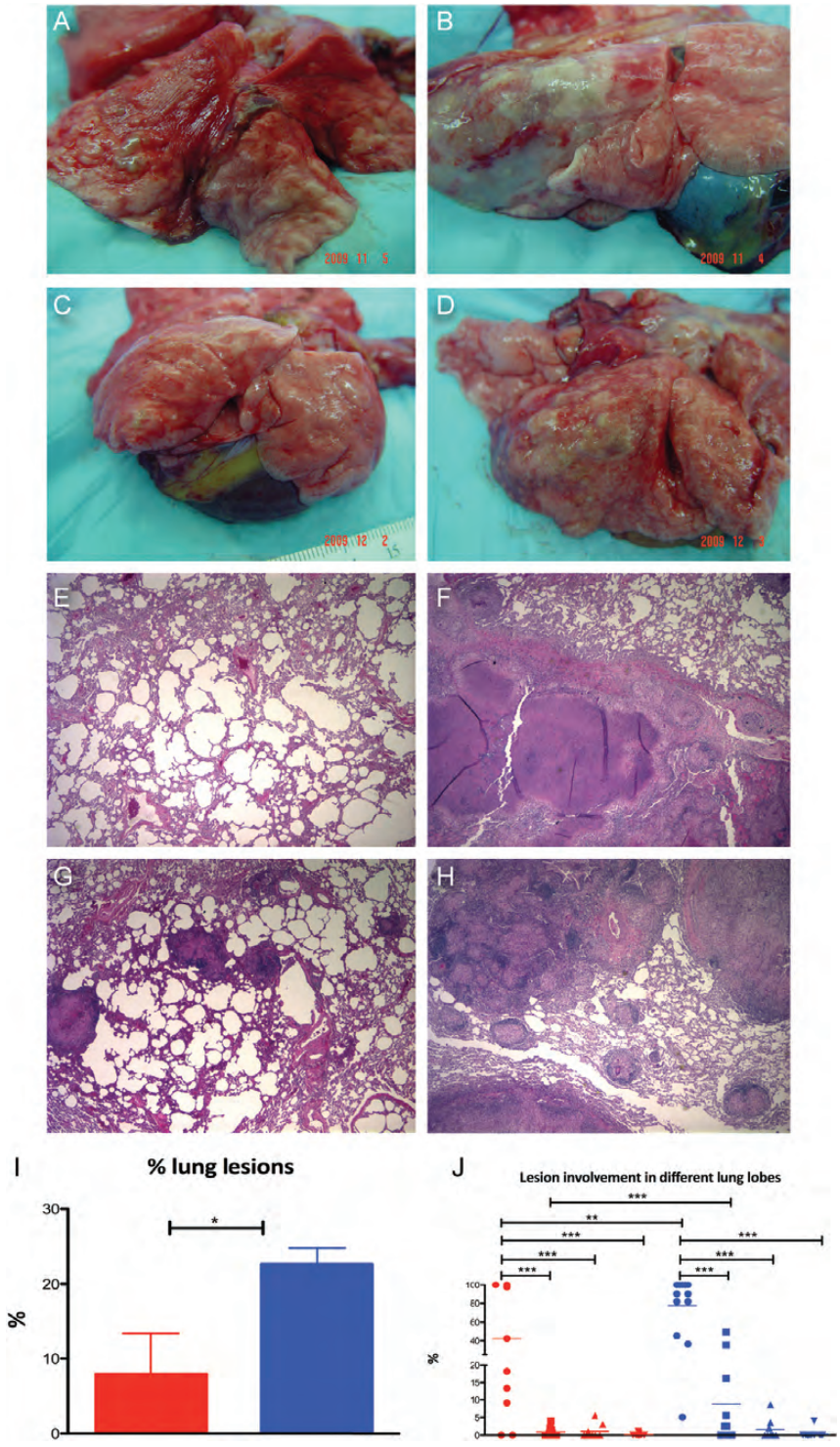

Figure 3. Comparison of pathology in sham and BCG-vaccinated nonhuman primates (NHPs). *A* and *C*, Gross pathology of lungs at necropsy from 2 representative BCG-vaccinated NHPs (*A* = 5 weeks, *C* = 10 weeks). *B* and *D*, Gross pathology of lungs at necropsy from sham-vaccinated NHPs (*B* = 5 weeks, *D* = 10 weeks). *E* and *G*, Histopathological analysis of hematoxylin-and-eosin (H&E)–stained lung sections from 2 representative BCG-vaccinated NHPs (*E* = 5 weeks, *G* = 10 weeks). *F* and *H*, Histopathological analysis of H&E-stained lung sections from 2 representative sham-vaccinated NHPs (*F* = 5 weeks, *H* = 10 weeks). *I*, Percentage of lung area involved in granulomatous lesions, edema, and consolidation relative to total lung area used for morphometric analysis. Red bar corresponds to BCG-vaccinated NHPs and blue bar corresponds to sham-vaccinated NHPs. *J*, Percentage of lung area (total as well as for individual animals) grouped into samples from lower right lobe (circles), all other lobes of right lung excluding the lower lobe (squares), contralateral left lower lobe (triangles facing up), and all other lobes of the left lung excluding the lower lobe (triangles facing down). Red symbols correspond to BCG-vaccinated and blue symbols correspond to sham-vaccinated NHPs.

Table 1. Immune Function Genes With Significantly Induced Expression in Lung Granulomas Isolated From Sham-Vaccinated Nonhuman Primates Relative to Normal Nongranulomatous Tissue at 5 and 10 Weeks After Infection

Category	Sham-Vaccinated/*Mycobacterium tuberculosis* (Week 5)	Sham-Vaccinated/*Mycobacterium tuberculosis* (Week 9)
Interferon	**INDO** (121.7), **STAT1** (12.8), TAP1 (10.6), **GBP1** (10.4), IFI30 (9.8), IRF1 (6.5), PSMB8 (4.7), IFN-γR2 (4.3), **IFN-γ** (3.8), IRF8 (3.2)	**INDO** (25.5), **IFN-γ** (11.5), **GBP1** (11), **STAT1** (7.1)
Tumor necrosis factor	**TNFSF13B** (10.3), **LITAF** (7.6), LTB (3.8), TNIP2 (3.1)	**TNFSF13B** (5.4), **LITAF** (3.5), LTA (3.1)
Chemokine	CXCL6 (21.8), **CXCL1** (19.7), **CXCL3** (14.5), **CXCL10** (10.9), **CXCL9** (9.6), CCL2 (8.3), CXCL14 (4.2), **CCL19** (3.9), CCL11 (3.5)	CXCL11 (29), **CXCL1** (26.5), **CXCL10** (14.5), CXCL13 (10), **CXCL3** (9.7), **CXCL9** (7.1),CXCL16 (4.7), **CCL19** (4.3)
Proinflammatory cytokines	IL1B (12.8), IL6 (12.1), IL1RN (3.4)	
Anti-inflammatory cytokines	IL4R (4.9), **IL10** (3.4), IL10RA (3.4)	IL10RB (6.1), **IL10** (4.7)
Innate immunity	**C1QA** (16.6), **APOL1** (13.3), KYNU (10.8), APOBEC3G (9.2),**TLR2** (9.0), **CYBB** (8.9), **IER3** (8.6), C3 (7.2), C1S (6.8),GCH1 (5.9), **ITGAM** (5.8), SERPING1 (5.2), C1QBP (4.1),C1QB (4.1), C2 (3.6), **TLR8** (3.4), **NCF2** (3.2)	**TLR2** (8.3), **CYBB** (7.8), **TLR8** (4.5), **ITGAM** (9.5), CR2 (8.7), **C1QA** (4.7), **APOL1** (4.1), **IER3** (3.1), **NCF2** (3)
Defense response	LYZ (85.3), TFRC (16), HLA-DRA (14.8), **RNASE3** (11.2),**CD74** (11), TAP1 (10.6), **LY96** (10), CD14 (9.1), TF (8.1), PSG4 (8), ITGB2 (7.3), B4GALT1 (6.7), **VSIG4** (6.6), CLIC1 (6.5), HIST1H2BK (6.4), CD48 (6.3), FGR (6.2), SERPINA1 (5.9),FN1 (5.7), TAPBP (5.1), NMI (4.8), SELS (4.6), CD44 (4.6),PLA2G4C (4.6), COTL1 (4.5), LYN (4.2), CD97 (3.9), **CD83** (3.6),ITGB1 (3.6) S100A8 (3.5), CEBPB (3.4), SPP1 (3.3),VDAC3 (3.3), TYROBP (3.1), **AOAH** (3.1), VDAC1 (3.1)	PLA2G7 (11.3), **VSIG4** (6.4), LY86 (6.1), **RNASE3** (5.6), **LY96** (5.1), **AOAH** (5.1), SLAMF8 (4.5), **CD83** (4.3),HMOX1 (4.0), **CD74** (3.3.), LY75 (3.2)
Apoptosis	**CTS**B (42.5), CD74 (11), **MMP9** (8.8), **CASP4** (8.2), **SEMA4D** (6), **BIRC3** (5.6), TPT1 (5.3), UBB (4.9), LGALS1 (4.7), CD44 (4.6), CASP1 (4.5), **ANXA4** (4.4), GFBP3 (4.4), BTG1 (4.1), HBXIP (4.1),CYCS (4), RPL11 (3.9), GPR109A (3.8), **SOD2** (3.8), CASP3 (3.7),CD2 (3.6), CEBPB (3.4), RPS27A (3.3), NME2 (3.3), NPM1 (3.2),CFL1 (3.2), PYCARD (3.1), MCL1 (3.1), PDCD5 (3.1), RPS6 (3.1)	**SOD2** (32.2), **MMP9** (25.7), BCL11B (7.9), **CTSB** (7.9),JAK2 (7.6), VDR (7), CHST11 (6.2), **BIRC3** (5.1),KCNMA1 (5.1), CDH1 (4.3), PPT1 (4.1), BCL10 (3.9),CALR (3.8), **SEMA4D** (3.5), **CASP4** (3.4), ACTN1 (3),CARD14 (3), CDKN1B (3), MAP3K5 (3),**ANXA4** (3)

Official National Center for Biotechnology Information human gene symbols are used to denote genes. Numbers in parentheses signify the numeric fold-change of expression for that gene. Functional groupings were constructed using DAVID (http://david.abcc.ncifcrf.gov/). Genes in boldface were present in the data set at both time points.

transcriptome profiles relative to normal lung tissue from uninfected animals. We first analyzed the gene expression in granulomatous lesions in sham-vaccinated NHPs that were euthanized at week 5, comparable to the transcriptome profiles of tuberculosis lesions from rhesus macaques infected via aerosol with a high-dose of *Mycobacterium tuberculosis* CDC1551 [8]. The early lesions in that study were characterized by the extremely high expression of proinflammatory genes. The expression of a majority of proinflammatory genes induced in rhesus macaques lesions were also induced in these lesions derived from cynomolgus macaques 5 weeks postinfection (Table 1). Numerous α-chemokines (but only 2 β-chemokines), cytokines, and interferon (IFN)– and tumor necrosis factor (TNF)–related genes exhibited induced expression in early tuberculosis lesions. The expression of many genes involved in innate immunity and defense as well as apoptosis was also induced, indicating the advent of the acute granulomatous response. Hence, the expression pattern of the early tuberculosis lesions remains proinflammatory, irrespective of the dose, inoculum, *Mycobacterium tuberculosis* strain, and route of infection.

Gene Expression in Late NHP Granulomas

Next we analyzed gene expression in tuberculosis lesions at week 10. The proinflammatory nature of the week 5 response was blunted in week 10 tuberculosis lesions (Table 1). However, the extent of transcriptional downregulation in this instance occurred to a lesser extent than in the rhesus study [8]. This was likely due to the fact that we analyzed granuloma expression at week 10 rather than week 13. Moreover, a significantly lower dose of *Mycobacterium tuberculosis* was used in this instance, in comparison to the experiment involving rhesus macaques. Hence, the progression to acute tuberculosis in the current study occurred less rapidly. None of the proinflammatory cytokines exhibited induced beyond 3-fold relative to normal lung tissues. Both the total number of genes induced and their magnitude of expression were lower for IFN-, TNF-, innate immune–, and defense-related genes

Table 2. Immune Function Genes With Significantly Induced Expression in Lung Granulomas Isolated From BCG-Vaccinated Nonhuman Primates Relative to Normal Nongranulomatous Tissue at 5 and 10 Weeks After Infection

Category	BCG-Vaccinated/*Mycobacteriumtuberculosis* (Week 5)	BCG-Vaccinated/*Mycobacteriumtuberculosis* (Week 9)
Interferon	**IFN-γ** (30.2), **INDO** (22.6), GBP1 (17.3), GBP2 (7.1), IRF1 (6.1), IFRG28 (5.2), IFI30, **STAT1** (5.1), FASLG (4.9), IL18 (4.7),IRF7 (4.2), IRF8 (3.8), ISG20 (3.5), STAT5A (3)	**INDO** (7.8), **STAT1** (5.9)
Tumor necrosis factor	LTB (9.8), **TNFSF13B** (8.6), TNFRSF11B, TNIP3 (7), **C1QTNF** (6.8), TNFAIP6 (6.5), TNFAIP3 (6), TNFRSF21 (5.9),TRAF3 (5.6), LTA (5.3), TNFAIP8 (3.5), TNFSF5 (3.2), TNIP2,TNF (3)	**TNFSF13B** (5.3), LITAF (3.6), **C1QTNF**, LTB (3)
Chemokine	**CXCL6** (57.3), CXCL9 (47.1), **CCL2** (38.2), CXCL11 (38.2),CXCL10 (37.4), CXCL1 (31.8), CXCL3 (18.2), **CCL19** (11.2),**CXCL13** (9.8), CCR1 (8.2), CXCL12 (7.6), CXCL14 (7.5),**CXCR4** (7.2), CCR5 (5.8), CXCL2 (5.5), CCL11 (5.3), CCR2(4.1), CXCL16 (4), CCL13 (3.9), CCR7 (3.5), CCL20, CCL4 (3)	**CXCL6** (11.1), **CXCL13**, **CXCR4** (5.7), **CCL2** (5.6), **CCL19** (4)
Proinflammatory cytokines	IL6 (69.2), IL1R2 (12.5), IL1B (12.4), IL15RA (6.9), IL1RAP (6.1), IL18RAP (5.3), IL21R, IL18R1 (4.7), IL2RA (4.5), IL27RA (3.4), IL12RB2 (3.1)	
Anti-inflammatory cytokines	IL10 (13), IL4I1 (10), IL11 (7.8), IL4R (4.4), IL10RA (3.8), SOCS1 (3.6), **IL10RB** (3.5)	IL4R (4.5), **IL10RA** (4.4), IL13RA1 (3.3)
Innate immunity	VSIG5 (16.8), TLR4 (10.2), CR2 (9.1), **IER3** (9), LAG3 (8.2), TLR2 (7.3), C4B (5.6), TLR8 (5.1), IRAK2 (4.2), **C1S** (4.5), **C4BPA**(3.8), C1QB (3.3), **C1QA** (3.2), **MYD88** (3)	C3 (6.7), **C1QA** (5.6), **C1S** (5.7), **C4B** (5), **IER3** (4.7), **C4BPA** (3), **MYD88**, NFKBIA (3)
Defense response	**MMP1** (84.1), INHBA (47.3), **SPP1** (37.9), SAA1 (36.7), SAA2 (34.3), S100A8 (33.2), SLAMF7 (29.1), HP (18.9), KYNU (16.5), SERPINA3 (15.3), SAA4 (14.9), ANKRD1 (13.3), GCH1 (10.1), CSF3R (9.7), **TFRC** (8.5), **CYBB** (8.3), **LYZ** (8.1), AOAH, GAL (7.8), IGFBP4, THBS1 (7.4), RNASE3,SERPINA1 (6.7), APOL2 (6.4), **APOL1**, SERPINF2 (5.7),**LY86** (5.5), APOL3, ORM1 (5), PLA2G7, KCNN4 (4.9), LY96 (4.5), B4GALT1, TAP1 (4.4), **PSG4** (4.3) RNASE6, PLA2G4C(4.2), HMOX, **CD48** (4.1), PTX3, LYN, RIPK2 (4), CD44 (3.9), APOBEC3G (3.8), ADORA2B, PTAFR (3.7), **CD83** (3.5), FGR(3.4), CYBA, **CLIC1** (3.1), CLEC5A, CD40, NOX1, AIF1, **SELS**(3)	**MMP1** (12.5), **APOL1** (10.1), **LYZ** (8.8), CD74 (8.2), **SPP1** (7.8), FN1 (7.6), B4GALT1 (7), TAP1 (6.1),HLA-DRA (6), SERPINA3 (4.7), **CD48** (4.6), **TFRC** (4.3), **CLIC1**, COTL1 (4.1), **CYBB** (3.9), **LYN** (3.8), SERPINA1 (3.6), **LY86** (3.5), **SELS** (3.4), LTA4H (3.3),**CD83**, **PSG4** (3.2), BLNK, FGR, MNDA, NMI, VDAC3(3)
Apoptosis	SOD2 (29.7), BID (14.2), GPR109A (13.3), GREM1 (12.6), SFRP5 (9.5), GPR65 (8), EGLN3, THBS1 (7.5), SGTB (6.2),DDIT4 (6), STEAP3 (5.8), **BIRC3**, TWIST1 (5.7), ZC3H12A(5.5), PHLDA2 (5.1), FADD (4.9), FASLG (4.7), OSM (4.5),**CASP4** (4.1), BCL2L14, SGPL1 (3.9), CYCS, JAK2 (3.4),BNIP2, **CD14**, GADD45A, **ITGB2**, **SIAH2**, UNC5B (3.2),ALDOC, NEK6, PYCARD (3)	PIM2 (8.1), CTNNB1 (6.5), **SIAH2** (5.2), **ITGB2**, RASSF5 (4.6),**BIRC3**, MAGEH1 (3.8), POLR2G (3.5), **CD14**, PREX1,YWHAE (3.4), MCL1, RTN4 (3.3), **CASP4** (3.2), YWHAB (3.1), MAP3K1 (3)

Official National Center for Biotechnology Information human gene symbols are used to denote genes. Numbers in parentheses signify the numeric fold-change of expression for that gene. Functional groupings were constructed using DAVID (http://david.abcc.ncifcrf.gov/).

(Table 1). Notably, the expression of MMP1 (66-fold), SOD2 (32-fold), MMP9 (26-fold), IDO (22-fold), etc, continued to be highly elevated.

Impact of BCG Vaccination on Gene Expression in NHP Granulomas

Next we analyzed gene expression in the lesions obtained from the lungs of animals that had been BCG-vaccinated 17 weeks prior to *Mycobacterium tuberculosis* challenge. The expression of numerous members of the IFN and TNF networks was induced in these lesions (Table 2). In particular, the expression of IFN-γ was induced >30-fold, despite the lower *Mycobacterium tuberculosis* burden in the lungs of this group of NHPs. In contrast, despite the higher bacillary burden in the sham-vaccinated NHPs, IFN-γ levels were induced <4-fold (Table 1). The levels of IFN-γ increased to approximately 11-fold in the late (week 10) lesions derived from the sham-vaccinated NHPs. Thus, BCG induces a memory response resulting in an early and substantially increased IFN-γ expression at the site of infection.

The expression of IFN-γ, CCL2, and IDO was assessed via gene-specific primer pairs using the CyBr-green method to confirm microarray results by quantitative reverse transcription–polymerase chain reaction. The expression of these genes was found to be consistent with microarray results (not shown).

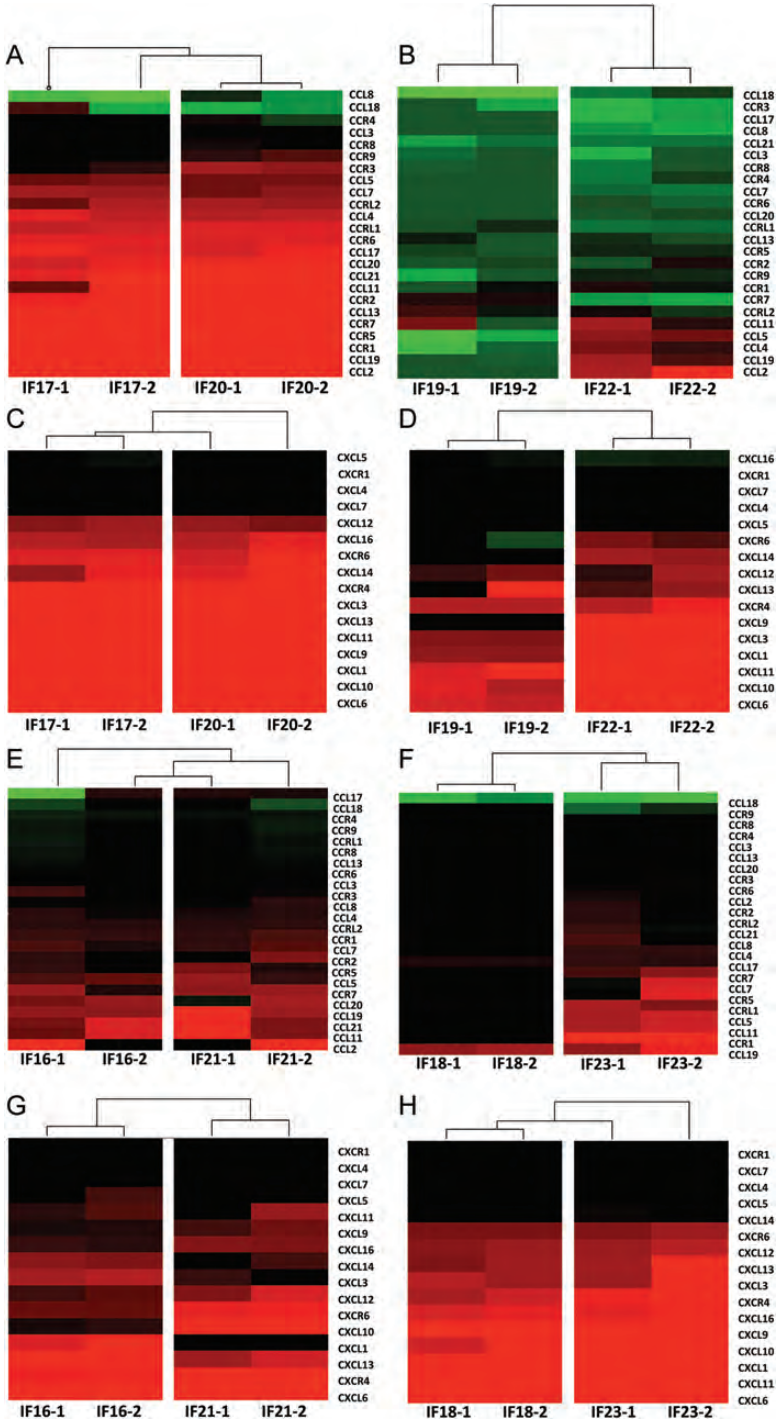

Figure 4. Microarray analysis of chemokine expression in BCG- and sham-vaccinated nonhuman primates (NHPs). Two individual (biological replicate) microarray experiments were performed for each of the 8 NHPs (IF17 and IF20 were BCG-vaccinated and euthanized 5 weeks after *Mycobacterium tuberculosis* infection; IF16 and IF21 were BCG-vaccinated and euthanized 10 weeks after *Mycobacterium tuberculosis* infection; IF19 and IF22 were sham-vaccinated and euthanized 5 weeks after *Mycobacterium tuberculosis* infection; and IF18 and IF23 were sham-vaccinated and euthanized 10 weeks after *Mycobacterium tuberculosis* infection), each including 3 granuloma lesion samples pooled together and compared to normal lung. *A*, Fold change for β-(CCL) chemokines and their receptors is shown for the BCG-vaccinated 5-week group of animals. *B*, Fold change for β-(CCL) chemokines and their receptors is shown for the sham-vaccinated 5-week group of animals. *C*, Fold change for β-(CXCL) chemokines and their receptors is shown for the BCG-vaccinated 5-week group of animals. *D*, Fold change for α-(CXCL) chemokines and their receptors is shown for the sham-vaccinated 5-week group of animals. *E*, Fold change for β-(CCL) chemokines and their receptors is shown for the BCG-vaccinated 10-week group of animals. *F*, Fold change for β-(CCL) chemokines and their receptors is shown for the sham-vaccinated 10-week group of animals. *G*, Fold change for α-(CXCL) chemokines and their receptors is shown for the BCG-vaccinated 10-week group of animals. *H*, Fold change for α-(CXCL) chemokines and their receptors is shown for the sham-vaccinated 10-week group of animals. Clustering was performed using Spotfire DecisionSite for Functional Genomics. The coloring scheme for the hierarchical cluster is as follows: black, no change in expression; green, lower expression in lesion samples relative to normal lung; and red, higher expression in lesion samples relative to normal lung. The intensity of red or green color corresponds to the extent of up- or downregulation.

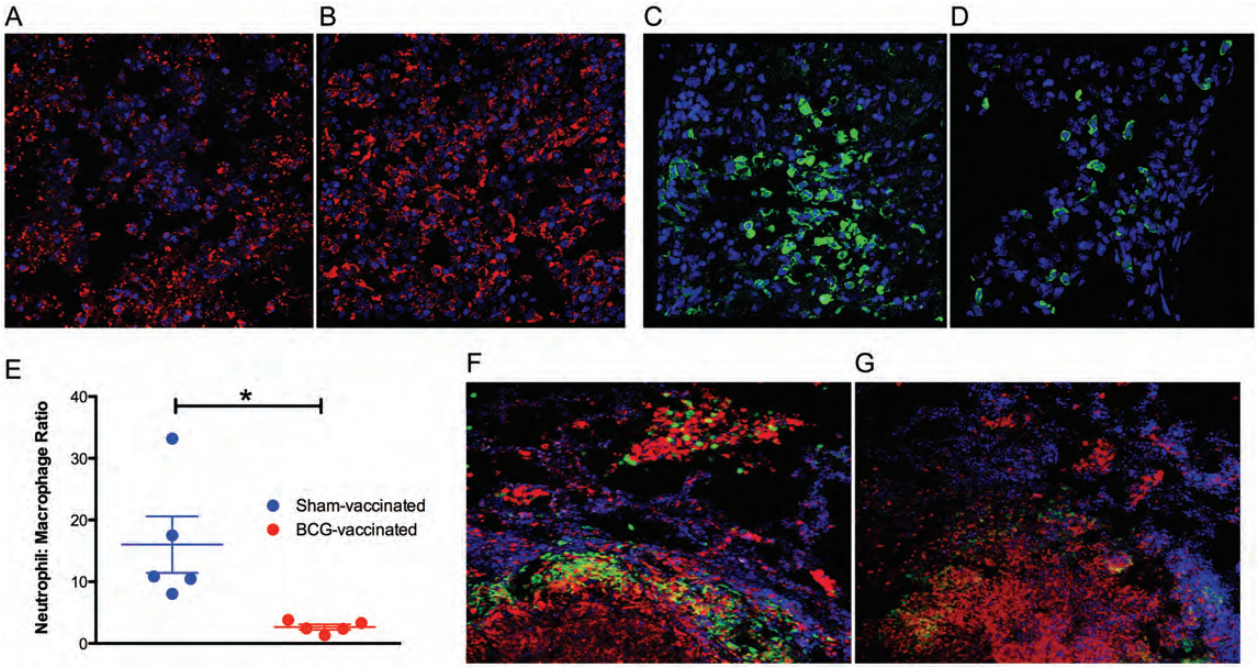

Figure 5. Confocal microscopy interrogation of tuberculosis granulomas in sham- and BCG-vaccinated nonhuman primates (NHPs). Staining for macrophages ($CD68^{+}$ $MAC387^{+lo}$; red) in lesions derived from a representative animal in the week 5 sham-vaccinated (*A*) and BCG-vaccinated (*B*) NHPs. Staining for neutrophils ($CD68^{-}$ $MAC387^{+hi}$; green) in lesions derived from a representative animal in the week 5 sham-vaccinated (*C*) and BCG-vaccinated (*D*) NHPs. Nuclei (blue) are stained with TOPRO-3. *E*, Neutrophil:macrophage count ratio from different lesions in the 2 groups. Staining for indoleamine 2,3-dioxygenase (green) and macrophages ($CD68^{+}$ $MAC387^{+lo}$; red) in lesions derived from a representative animal in the week 5 sham-vaccinated (*F*) and BCG-vaccinated (*G*) NHPs. Again, nuclei are stained with TOPRO-3.

Differential Induction of α- and β-Chemokines in Granulomas Derived From BCG-Vaccinated vs Sham-Vaccinated NHPs

The expression of several chemokine genes was enhanced following *Mycobacterium tuberculosis* infection in BCG-vaccinated NHPs. However, in this instance, several β-chemokine genes (CCL2, 4, 11, 13, 19, 20) were also induced in addition to α-chemokine genes (CXCL1, 3, 6, 9, 10, 11, 13, 16). Several β-chemokine receptor genes also exhibited increased expression (CCR1, 2, 5, and 7; Table 2). The enhanced expression of β-chemokines was in contrast to lesions obtained from the sham-vaccinated, *Mycobacterium tuberculosis*-infected macaques (Figure 4). This was especially evident in the early (week 5) lesions (Figure 4*A* and 4*B*). In samples derived from sham-vaccinated macaques, few β-chemokine genes (CCL2, 11) and no β-chemokine receptor genes showed consistent induction. Of the β-chemokine genes that were induced in both BCG- and sham-vaccinated NHPs, the magnitude of CCL2 (38-fold relative to 8-fold) and CCL11 (5-fold relative to 3-fold) expression was also higher in the former, relative to the latter group. The expression of α-chemokines was induced to high levels in the early lesions derived from both groups of animals (Figure 4*C* and 4*D*). The expression of CXCL16, CXCR6, CXCL14, CXCL13, and CXCL9 was, however, slightly higher in early lesions from BCG- rather than sham-vaccinated animals, though the differences, both in magnitude and breadth, were nowhere near those observed for β-chemokines. Thus, the expression of β-chemokines and the recruitment to the lung of cells in response to this signal correlates with protection, while the production of α-chemokines alone, in the absence of β-chemokines, correlates with disease progression.

Lesions From Unvaccinated Animals Contain Fewer Macrophages

The α-chemokines CXCL1, CXCL2, CXCL3, CXCL6, and CXCL8 are major chemoattractant factors for neutrophils [17–21]. In contrast, β-chemokines are mainly responsible for macrophage and lymphocyte recruitment and homing (CCL2, CCL3, CCL4, CCL5, CCL13, CCL19, CCL21) [22–25]. Because lesions from sham-vaccinated NHPs expressed primarily α-chemokines, whereas those from BCG-vaccinated NHPs expressed a better balance of both α- and β-chemokines, we assessed if fewer macrophages (or more neutrophils) are recruited to the lungs of unvaccinated primates or conversely if more macrophages (or fewer neutrophils) are recruited to the lungs of BCG-vaccinated animals following the challenge. To discriminate between macrophages and neutrophils, a multispectral

microscopy strategy was devised. Macrophages in nonhuman primate lungs are mainly $CD68^+$ whereas granulocytes are highly positive for $MAC387^+$. Monocytes can also present MAC387, albeit at lower level [26]. Thus, neutrophils were identified by $MAC387^{+hi}$ while $CD68^+$ $MAC387^{+low}$ cells were phenotyped as macrophages. Week 5 lesions from vaccinated animals harbored significantly more macrophages, relative to comparable lesions from the unvaccinated animals (Figure 5*A* and 5*B*). The total number of neutrophils detected in lesions derived from unvaccinated animals was higher than in lesions from the unvaccinated animals (Figure 5*C* and 5*D*). Thus, the lesion neutrophil:macrophage ratio was significantly higher for unvaccinated relative to vaccinated animals (Figure 5*E*). These results are in accordance with the observed expression of chemokines in the lesions from the 2 groups (Figure 4). Further, these results confirm the growing understanding that acute progression of *Mycobacterium tuberculosis* infections and the concomitant immunopathology correlates with decreased macrophage and increased neutrophil recruitment in humans [27] and mice [28].

IDO Expression is Highly Induced in Tuberculosis Lesions

The expression of IDO was induced approximately 122-fold in early lesions derived from sham-vaccinated NHPs (Table 1). In contrast, the expression of IDO was induced approximately 22-fold in week 5 lesions derived from BCG-vaccinated NHPs (Table 2). Similarly, the expression of IDO in late (week 10) lesions from the vaccinated NHPs was significantly lower than in the time-matched lesions from the unvaccinated animals (8-fold vs 26-fold). The expression of IDO in early (week 5) BCG-vaccinees was comparable to that in late (week 10) tuberculosis lesions (22-fold vs 26-fold), indicating that the expression of this gene was reduced over the course of time from peak in both groups of NHPs. Thus, in the absence of protective vaccination, the expression of IDO was increased to significantly higher levels and much earlier in time. Recent reports have shown that *Mycobacterium tuberculosis* infection of macrophages in vitro [15, 29] and in vivo [8] induces IDO expression. It is being proposed that IDO is part of a deliberate immune subversion mechanism by intracellular pathogens [30].

Expression of IDO Occurs in the Ring-Wall Regions of NHP Tuberculosis Granulomas

Multilabel confocal immunofluorescence was used to verify the differential expression of IDO in the lung lesions of vaccinated and sham-vaccinated animals. The expression of IDO was detected in all samples studied, but distinctly higher in samples derived from sham-vaccinated NHPs, thus confirming the transcriptomic results (Figure 5*F* and 5*G*).

Interestingly, the expression of IDO was at its greatest in cells lining the ring-wall (ie, the inner caseum of the granuloma lesions) and primarily occurred in larger cells (Figure 5*E–H*). Intense expression of IDO has been reported to occur in dendritic cells within the ring-wall structure of granuloma lesions formed following *Listeria monocytogenes* infection in humans [31]. Hence, we investigated whether the expression of IDO was also largely limited to this cell type and region with the tuberculosis granulomas. The expression of IDO in both groups of animals did not colocalize with dendritic cells (using a anti–dendritic cell SIGN antibody) in tuberculosis lesions (not shown). However, the expression of IDO largely occurred in the ring-wall structure of the tuberculosis granulomas, within the macrophage-rich region (Figure 5*E–H*). These extremely novel findings point to previously unknown mechanisms that are potentially utilized to control acute granulomatous immunopathology.

DISCUSSION

The long-term control of tuberculosis requires the development of efficacious vaccines. In turn, this requires a complete understanding of the bacterial mediators of virulence and host mediators of protection in appropriate animal models. Primate granulomas exhibit highly ordered architecture, mostly with central necrosis surrounded by a peripheral rim. Such lesions are thought to be critical for containing *Mycobacterium tuberculosis* replication, and conversely, permitting the latent survival program of the pathogen [5]. In fact, hypoxia and necrosis during human tuberculosis infections are likely to have such profound influence on the physiology of the pathogen that a study of host-*Mycobacterium tuberculosis* interaction in hosts with nonhypoxic granulomas [32] may be misleading [33]. Hence, characterization of primate granulomas allows a better understanding of the mediators of latency and reactivation.

We characterized the lung granulomas of primates with active tuberculosis, at an early and a late stage of infection, by transcriptomics and compared these results to those obtained from a similar investigation on animals that had been BCG-vaccinated prior to *Mycobacterium tuberculosis* challenge. Our contention was to generate a list of potential markers that may be able to predict either protection from lethal *Mycobacterium tuberculosis* challenge, or progression to acute disease, or both. Our study has generated several important results. We show that BCG vaccination significantly reduced the burden of tuberculosis in cynomolgus macaques. The vaccinated animals had significantly reduced bacterial load, clinical correlates of acute tuberculosis, and immunopathology. BCG vaccination significantly decreased the potential for the transmission of the bacilli from the primary site of infection to secondary lung sites, but did not protect against bolus infection with 250 CFU *Mycobacterium tuberculosis* Erdman at the primary locus.

Prior BCG vaccination had a substantial effect on the expression of chemokines, potentially impacting the structure and the composition of the granuloma, as chemokines orchestrate the migration of specific immune effector cells expressing their cognate receptors to the site of infection. The α-chemokines CXCL1, CXCL2, CXCL3, CXCL6, and CXCL8 are known to attract neutrophils, which express their cognate receptors CXCR2, CXCR3, and CXCR5 to high levels. The expression of these neutrophil-specific chemokines occurred at a comparable level in the lesions of both BCG- and sham-vaccinated NHPs. However, both the total number of and the magnitude of expression of β-chemokines were higher in lesions derived from vaccinated NHPs (Figure 4). The β-chemokines are responsible for macrophage and lymphocyte recruitment (CCL2, CCL3, CCL4, CCL5) and homing to tissues (CCL13, CCL19, CCL21). Hence, an important marker of protection against *Mycobacterium tuberculosis* infection may be the expression balance of α- and β-chemokines or the neutrophil:macrophage ratio in lung samples.

Neutrophils are the earliest responding cell type following *Mycobacterium tuberculosis* infection and have bactericidal function. However, there is mounting evidence that increased recruitment of neutrophils, relative to macrophages, to the lung following *Mycobacterium tuberculosis* infection causes uncontrolled immunopathology and is detrimental to the resolution of the disease [27, 34, 35], perhaps because of inhibition of macrophage antimycobacterial activity [36–38]. Our results, obtained using an appropriate model of human tuberculosis, support this hypothesis. Vaccinated animals exhibited fewer neutrophils and more macrophages, and a significantly lower neutrophil:macrophage ratio in their lung lesions.

IDO was most highly induced in the early lesions of sham-vaccinated macaques. IDO is responsible for tryptophan degradation in mammals [39]. Because tryptophan is an essential amino acid, ability to catabolize it represents a strategy by the immune system to starve pathogens by inducing the expression of IDO and the resulting depletion of tryptophan, for example, during infections with *Toxoplasma gondii* [40, 41].

However, evidence has recently emerged that IDO mediates powerful immunomodulatory functions downstream of IFN-γ [42] and TNF [31], by inhibiting T helper 1–type response due to tryptophan starvation [29]. Hence, the stimulation of IDO expression may constitute a strategy by some pathogens to create local immune privilege at the site of infection, which could in turn attenuate innate immune responses and allow pathogen replication.

IDO expression was highly induced by *Mycobacterium tuberculosis* infection, but to a significantly lower extent in vaccinated and protected NHPs. Thus, *Mycobacterium tuberculosis* may also utilize the immunomodulatory effects of IDO to further its replication. This notion is strengthened by the observation that IDO is almost exclusively expressed in the ring wall of granuloma lesions. Granuloma formation is a critical step toward the control of *Mycobacterium tuberculosis* infection. Neutrophils, macrophages, and lymphocytes are essential components of tuberculosis granulomas. Phagocytes are the major constituents of the ring walls of caseous tuberculosis granulomas. Concomitantly, lymphocytes are rarely present in the ring walls (Figure 5*F*–*G*). Because IDO generates a strong anti–T-cell inhibitory effect [31, 43–46], we propose that IDO in ring wall prevents activated T cells from accessing the pathogen in the central caseous region. This may be beneficial to the host, as infiltration of central granuloma region by T cells may potentially disrupt the lesion, thus allowing the escape of the pathogen.

There is evidence to support this notion. $Tnf^{-/-}$ mice are highly susceptible to *Mycobacterium tuberculosis* infections owing to extensive damage to the granuloma structure by an uncontrolled type 1 response [47]. When CD4 or CD8 T lymphocytes were selectively depleted, the damage to the granuloma structure was abrogated, translating into a prolonged survival of the susceptible $Tnf^{-/-}$ mice following challenge. In our current study, all NHPs exhibited induced levels of IDO in the ring walls of lung granulomas, but animals with prior BCG vaccination, which were protected from severe tuberculosis, exhibited several-fold lower IDO levels than animals with acute disease. Thus, the expression of IDO may be a lung protective mechanism.

Our model assigns a novel function to IDO in response to *Mycobacterium tuberculosis* infection that would require subsequent experiments in the future for validation. Mice commonly used for tuberculosis infections do not exhibit the highly organized structure of human or primate lung granulomas. Because murine granulomas do not caseate, it is unlikely that murine lesions will either exhibit such a morphologically defined expression of INDO. However, recent reports indicate that C3H:FeJ (Kramnik) mice develop necrotic granulomas [48]. It will be interesting to study the morphology of INDO expression in Kramnik mice infected with *Mycobacterium tuberculosis*.

Notes

Acknowledgments. We gratefully acknowledge Dr Sheldon Morris, Vaccine Research Center, Food and Drug Administration, for sharing BCG Danish and *Mycobacterium tuberculosis* Erdman stocks with us. We also acknowledge excellent technical assistance by Cecily C. Midkiff.

Author contributions. Design: S. M., D. K.; research: S. M., X. A.; data analysis: S. M., X. A., P. J. D., D. K.; writing: S. M., D. K.; pathology: P. J. D., A. A. L.; veterinary medicine: L. A. D., J. L. B.; funding: A. A. L., D. K.

Financial support. This work was supported by the National Institutes of Health (grant numbers AI089323, HL106790, AI091457, RR026006, RR020159, RR000164/OD011104, and C06AI058609) and the Louisiana Vaccine Center, Tulane Research Enhancement Fund, Tulane Center for Infectious Diseases, and Tulane Office of Vice-President for Research (Bridge Fund).

Potential conflicts of interest. All authors: No reported conflicts.

All authors have submitted the ICMJE Form for Disclosure of Potential Conflicts of Interest. Conflicts that the editors consider relevant to the content of the manuscript have been disclosed.

References

1. Dye C. Global epidemiology of tuberculosis. Lancet **2006**; 367:938–40.
2. Orme IM. Prospects for new vaccines against tuberculosis. Trends Microbiol **1995**; 3:401–4.
3. Orme IM. The Achilles heel of BCG. Tuberculosis **2010**; 90:329–32.
4. Russell DG. Who puts the tubercle in tuberculosis? Nat Rev Microbiol **2007**; 5:39–47.
5. Paige C, Bishai WR. Penitentiary or penthouse condo: the tuberculous granuloma from the microbe's point of view. Cell Microbiol **2010**; 12:301–9.
6. Kaushal D, Mehra S, Didier PJ, Lackner AA. The nonhuman primate model of tuberculosis. J Med Primatol **2012**; 41:191–201.
7. Kaushal D, Mehra S. Faithful experimental models of human *Mycobacterium tuberculosis* infections. Mycobacterial Dis **2012**; 2:1.
8. Mehra S, Pahar B, Dutta NK, et al. Transcriptional reprogramming in nonhuman primate (rhesus macaque) tuberculosis granulomas. PLoS One **2010**; 5:e12266.
9. Verreck FA, Vervenne RA, Kondova I, et al.. MVA.85A boosting of BCG and an attenuated, *pho*P deficient *M. tuberculosis* vaccine both show protective efficacy against tuberculosis in rhesus macaques. PLoS One **2009**; 4: e5264.
10. Larsen MH, Bierman K, Chen B, et al. Efficacy and safety of live attenuated persistent and rapidly cleared *Mycobacterium tuberculosis* vaccine candidates in non-human primates. Vaccine **2009**; 27:4709–17.
11. Gormus BJ, Blanchard JL, Alvarez XH, Didier PJ. Evidence for a rhesus monkey model of asymptomatic tuberculosis. J Med Primatol **2004**; 33:134–45.
12. Dutta NK, Mehra S, Didier PJ, et al. Genetic requirements for the survival of tubercle bacilli in primates. J Infect Dis **2010**; 201:1743–52.
13. Mehra S, Golden NA, Dutta NK, et al. Reactivation of latent tuberculosis in rhesus macaques by co-infection with simian immunodeficiency virus. J Med Primatol **2011**; 40:233–43.
14. Mehra S, Golden NA, Stuckey KJ, et al. The *Mycobacterium tuberculosis* SigH is required for bacterial burden as well as immunopathology in primates. J Infect Dis **2012**; 205:1203–13.
15. Dutta NK, Mehra S, Martinez AN, et al. The stress-response factor SigH modulates the interaction between *Mycobacterium tuberculosis* and host phagocytes. PLoS One **2012**; 7:e28958.
16. Kaushal D, Naeve CW. Analyzing and visualizing expression data with Spotfire. Curr Prot Bioinform **2004**; chapter 7, unit 7.9.
17. Schroder JM, Mrowietz U, Christophers E. Purification and partial biologic characterization of a human lymphocyte derived peptide with potent neutrophil-stimulating activity. J Immunol **1988**; 140:3534–40.
18. Huang S, Paulauskis JD, Godleski JJ, Kobzik L. Expression of macrophage inflammatory protein-2 and KC mRNA in pulmonary inflammation. Am J Pathol **1992**; 141:981–8.
19. Nakagawa H, Komorita N, Shibata F, et al. Identification of cytokine-induced neutrophil chemoattractants (CINC), rat GRO/CINC-2 alpha and CINC-2 beta, produced by granulation tissue in culture: purification, complete amino acid sequences and characterization. Biochem J **1994**; 301:545–50.
20. Schmal H, Shanley TP, Jones ML, Friedl HP, Ward PA. Role for macrophage inflammatory protein-2 in lipopolysaccharide-induced lung injury in rats. J Immunol **1996**; 156:1963–72.
21. Wuyts A, Van Osselaer N, Haelens A, et al.. Characterization of synthetic human granulocyte chemotactic protein 2: usage of chemokine receptors CXCR1 and CXCR2 and in vivo inflammatory properties. Biochemistry **1997**; 36: 2716–23.
22. Schall TJ. Biology of the RANTES/SIS cytokine family. Cytokine **1991**; 3:165–83.
23. Blanpain C, Migeotte I, Lee B, et al. CCR5 binds multiple CC-chemokines: MCP-3 acts as a natural antagonist. Blood **1999**; 94:1899–905.
24. Reif K, Ekland EH, Ohl L, et al. Balanced responsiveness to chemoattractants from adjacent zones determines B-cell position. Nature **2002**; 416:94–9.
25. Weninger W, von Andrian UH. Chemokine regulation of naïve T cell traffic in health and disease. Semin Immunol **2003**; 15:257–70.
26. DeJesus CE, Egen J, Metzger M, et al. Transient neutropenia after granulocyte-colony stimulating factor administration is associated with neutrophil accumulation in pulmonary vasculature. Exp Hematol **2011**; 39:142–50.
27. Eum SY, Kong JH, Hong MS, et al. Neutrophils are the predominant infected phagocytic cells in the airways of patients with active pulmonary TB. Chest **2010**; 137:122–8.
28. Eruslanov EB, Lyadova IV, Kondratieva TK, et al. Neutrophil responses to *Mycobacterium tuberculosis* infection in genetically susceptible and resistant mice. Infect Immun **2005**; 73:1744–53.
29. Blumenthal A, Nagalingam G, Huch JH, et al.. *M. tuberculosis* induces potent activation of IDO-1, but this is not essential for the immunological control of infection. PLoS One **2012**; 7:e37314.
30. Schmid M, Lehmann MJ, Lucius R, Gupta N. The apicomplexan parasite, *Eimeria falciformis*, co-opts host tryptophan catabolism for life cycle progression in the mouse. J Biol Chem **2012**; 287:20197–207.
31. Popov A, Abdullah Z, Wickenhauser C, et al. Indoleamine 2,3-dioxygenase-expressing dendritic cells form suppurative granulomas following *Listeria monocytogenes* infection. J Clin Invest **2006**; 116: 3160–70.
32. Via LE, Lin PL, Ray SM, et al. Tuberculous granulomas are hypoxic in guinea pigs, rabbits, and nonhuman primates. Infect Immun **2008**; 76:2333–2340.
33. Kaufmann SH, Cole ST, Mizrahi V, Rubin E, Nathan C. *Mycobacterium tuberculosis* and the host response. J Exp Med **2005**; 201:1693–97.
34. Kondratieva E, Logunova N, Majorov K, Averbakh M, Apt A. Host genetics in granuloma formation: human-like lung pathology in mice with reciprocal genetic susceptibility to *M. tuberculosis* and *M. avium*. PLoS One **2010**; 5:e10515.
35. Love DM, Redford PS, Wilkinson RJ, O'Garra A, Martineau AR. Neutrophils in tuberculosis: friend or foe? Trends Immunol **2012**; 33:14–25.
36. Kondratieva TK, Rubakova EI, Linge IA, Evstifeev VV, Majorov KB, Apt AS. B cells delay neutrophil migration toward the site of stimulus: tardiness critical for effective bacillus Calmette-Guérin vaccination against tuberculosis infection in mice. J Immunol **2010**; 184: 1227–34.
37. Sawant KV, Cho H, Lyons M, Ly LH, McMurray DN. Guinea pig neutrophil-macrophage interactions during infection with *Mycobacterium tuberculosis*. Microbes Infect **2010**; 12:828–37.
38. Duarte TA, Noronha-Dutra AA, Nery JS,, et al. *Mycobacterium tuberculosis*-induced neutrophil ectosomes decrease macrophage activation. Tuberculosis (Edinb) **2012**; 92:218–25.
39. Taylor MW, Feng GS. Relationship between interferon-gamma, indoleamine 2,3-dioxygenase, and tryptophan catabolism. FASEB J **1991**; 5:2516–22.
40. Pffefferkorn ER. Interferon gamma blocks the growth of *Toxoplasma gondii* in human fibroblasts by inducing the host cells to degrade tryptophan. Proc Natl Acad Sci U S A **1984**; 81:908–12.
41. Thomas SM, Garrity LF, Brandt CR, et al. IFN-gamma-mediated antimicrobial response. Indoleamine 2,3-dioxygenase-deficient mutant host cells no longer inhibit intracellular *Chlamydia* spp. or *Toxoplasma* growth. J Immunol **1993**; 150:5529–34.
42. Loughman JA, Hunstad DA. Induction of indoleamine 2,3-dioxygenase by uropathogenic bacteria attenuates innate responses to epithelial infection. J Infect Dis **2012**; 205:1830–9.
43. Mellor AL, Munn DH. IDO expression by dendritic cells: tolerance and tryptophan catabolism. Nat Rev Immunol **2004**; 4:762–74.
44. von Bergwelt-Baildon MS, Popov A, Saric T, et al. CD25 and indoleamine 2,3-dioxygenase are up-regulated by prostaglandin E2 and expressed by tumor-associated dendritic cells in vivo: additional mechanisms of T-cell inhibition. Blood **2006**; 108:228–37.

45. Terness P, Bauer TM, Röse L, et al. Inhibition of allogeneic T cell proliferation by indoleamine 2,3-dioxygenase-expressing dendritic cells: mediation of suppression by tryptophan metabolites. J Exp Med **2002**; 196:447–57.
46. Munn DH, Sharma MD, Lee JR, et al. Potential regulatory function of human dendritic cells expressing indoleamine 2,3-dioxygenase. Science **2002**; 297:1867–70.
47. Zganiacz A, Santosuosso M, Wang J, et al. TNF-alpha is a critical negative regulator of type 1 immune activation during intracellular bacterial infection. J Clin Invest **2004**; 113:401–13.
48. Harper J, Skerry C, Davis SL, et al. Mouse model of necrotic tuberculosis granulomas develops hypoxic lesions. J Infect Dis **2012**; 205: 595–602.